Journal of Photonics for Energy

SPIEDigitalLibrary.org/jpe

Transparent oxide/metal/oxide trilayer electrode for use in top-emitting organic light-emitting diodes

Edward Wrzesniewski
Sang-Hyun Eom
William T. Hammond
Weiran Cao
Jiangeng Xue

SPIE

Transparent oxide/metal/oxide trilayer electrode for use in top-emitting organic light-emitting diodes

Edward Wrzesniewski, Sang-Hyun Eom, William T. Hammond, Weiran Cao, and Jiangeng Xue
University of Florida, Department of Materials Science and Engineering, Gainesville, Florida 32611–6400
jxue@mse.ufl.edu

Abstract. The most commonly used transparent electrode, indium-tin oxide (ITO), is costly and requires methods of deposition that are highly destructive to organic materials when it is deposited on top of the organic layers in top-emitting organic light-emitting devices (OLEDs). Here we have employed a trilayer electrode structure consisting of a thin layer of metal sandwiched between two MoO_3 layers, which can be deposited through vacuum thermal evaporation without much damage to the organic active layers. Such MoO_3/Au/MoO_3 trilayer electrodes have a maximum transmittance of nearly 90% at 600 nm and a sheet resistance of <10 ohms per square (Ω/sq) with a 10-nm thick Au intermediate layer. Using these trilayers as the top transparent anode, we have fabricated top-emitting OLEDs based on either a fluorescent or phosphorescent emitter, and observed nearly identical emission spectra and similar external quantum efficiencies as compared to the more conventional bottom-emitting OLEDs based on the commercial ITO anode. The power efficiency of the top-emitting devices is 20% to 30% lower than the bottom-emitting devices due to the somewhat inferior charge injection in the top-emitting devices. The performance and emission characteristics of these devices indicate that this trilayer structure is a promising candidate as a transparent anode in top-emitting OLEDs.
 [DOI: 10.1117/1.3592886]

Keywords: organic light-emitting diode; transparent electrode; metal oxide; top-emitting organic light emitting diodes; sheet resistance.

Paper 10160SSPR received Sep. 1, 2010; revised manuscript received Apr. 12, 2011; accepted for publication May 2, 2011; published online May 23, 2011.

1 Introduction

Organic light emitting diodes (OLEDs) are already commercially available in small-area displays and quickly approaching the point of commercial viability for lighting applications. White light devices with efficiencies reaching 100 lumens per watt (lm/W) have been achieved,[1] which exceed the maximum efficiencies of the incandescent (17 lm/W) and fluorescent bulbs (90 lm/W).[2] Soon flat panels with strong color rendering capabilities could replace conventional lighting fixtures both at home and in commercial environments. While these devices could one day revolutionize technology, one important component that still requires investigation is the transparent electrode, which must be conductive but also transparent so as to facilitate the transmission of light to and from the active organic layers. The most common transparent electrode used for these devices is indium-tin oxide (ITO), a degenerately doped metal oxide consisting of 90% In_2O_3 and 10% SnO_2, typically deposited in a sputtering system at elevated substrate temperatures to simultaneously optimize the optical transparency and electrical conductivity.[3,4] This electrode can be patterned onto glass or other transparent substrates, and has high transparency of approximately 90% across the visible spectrum and low sheet resistance of 10 to

1947-7988/2011/$25.00 © 2011 SPIE

20 ohms per square (Ω/sq) for a 100 to 150-nm-thick film; however, the high temperatures induced by the plasma, as well the necessary post-deposition annealing process, will cause the thermal expansion of polymer-based substrates and significantly reduce the conductivity of the layer.

Typically, OLEDs are designed to emit through ITO and the transparent substrate before reaching air (there is typically a metal electrode on the other side of the organic multilayer stacks to reflect the light toward the ITO electrode). This leads to three distinct interfaces which light must pass through: one between the organic layers and ITO, one between the ITO and glass, and one between glass and air. The differences in indices of refraction between these components mean that at each interface light has the potential to be internally reflected, reducing the overall efficiency of the device. If one could remove the interface between glass and substrate by switching the position of the transparent ITO electrode and the reflective metal electrode, light previously trapped internally in wave-guided modes could now partially escape the device.[5,6] This top-emitting structure, wherein the device emits directly from a transparent electrode to air, has the potential to improve the outcoupling of light[7,8] and drive organic devices toward higher efficiencies. Furthermore these devices can also be fabricated on opaque substrates like silicon, allowing for integration into current active matrix display technologies. Unfortunately, with respect to top-emitting organic devices, the ITO electrode does not easily integrate into the fabrication process due to its method of deposition. The sputtering process is highly destructive to the soft organic layers underneath.[9] Therefore, another transparent electrode is necessary for use in top-emitting or semitransparent organic devices.

Recently, the use of multilayer patterned electrodes consisting of thin metal layers sandwiched by oxide layers has been investigated.[10–14] While these electrodes have typically been deposited using e-beam deposition and therefore require additional processing steps and chambers apart from traditional thermal evaporation, Yook et al. have shown that such a structure can be thermally evaporated as well, which integrates into the fabrication of small molecule organic devices and has less potential to damage the underlying layers.[12] Typically the metal used has been Ag, while the oxide layers have run the gamut from ITO to WO_3 to ZnO.

Our work seeks to expand the understanding of these multilayer electrode structures, and their integration into top-emitting diode design for high efficiency OLEDs. Previously the use of Ag as the intermediate layer showed a wavelength dependent transmittance favoring the blue region (400 to 500 nm) of the visible spectrum, and the application of this structure as a cathode in place of the typical Al or Ag.[10] By contrast, replacing this layer with Au and sandwiching it between layers of molybdenum oxide (MoO_3), we have shown a shift in peak transmittance toward the green and red regions (550 to 600 nm) of the spectrum, while maintaining a low sheet resistance. Furthermore, when ultrathin layers of Au and Ag are stacked in this structure, the peak transmittance can be both broadened and tuned based on the proportions of each layer. Finally, the structure was incorporated as an anode into OLED devices showing the potential for high efficiency devices with an inverted top-emitting structure.

2 Experimental

All structures were deposited on glass substrates using vacuum thermal evaporation at a pressure $< 3.0 \times 10^{-6}$ Torr. The substrates were cleaned by submerging the samples in beakers of detergent and water, de-ionized water, acetone, and isopropanol successively, and each beaker was ultrasonicated for a period of 15 min. The transparent oxide/metal/oxide structures were deposited sequentially using 5 nm of MoO_3 followed by various thicknesses of Au or Ag and finally 40 nm of MoO_3. OLEDs were then fabricated using an inverted top-emitting structure and compared to a standard bottom-emitting architecture deposited on top of a precoated ITO layer. Figure 1 illustrates these two different structures. Both fluorescent and phosphorescent devices were examined. The fluorescent structure consisted of *N*,*N*′-diphenyl-*N*,*N*′-bis(3-methylphenyl)-[1,1′-biphenyl]-4,4′-diamine (MeO-TPD) doped with tetrafluoro-tetracyanoquinodimethane (F_4-TCNQ) as the hole injecting layer (HIL),[15] *N*,*N*′-

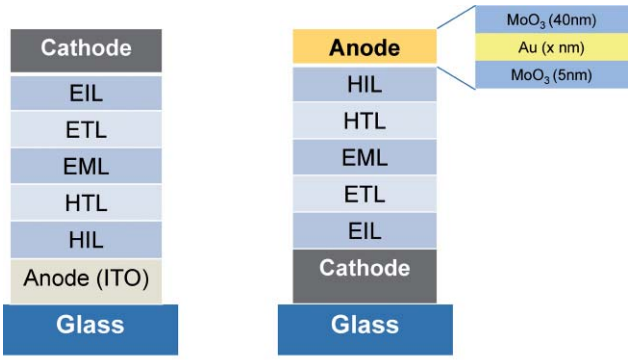

Fig. 1 Schematic device structures for the standard bottom-emitting architecture (a) based on the commercial ITO electrode and the top-emitting architecture (b) based on the MoO_3/metal/MoO_3 trilayer transparent electrode.

bis-(1-naphthyl)-*N*,*N*′-diphenyl1–1,1-biphenyl1–4,4′-diamine (NPB) as a hole transporting layer (HTL),[16] and tris(8-hydroxyquinolinato) aluminum (Alq_3) as the electron transport (ETL) and emitting layer (EML).[17] The respective transparent electrodes (ITO for bottom-emitting devices and the oxide/metal/oxide trilayer for top-emitting devices) were used as the anodes, whereas a Cs_2CO_3 interlayer[18] and Al were used as the cathode. Phosphorescent devices consisted of a *p-i-n* structure with MeO-TPD doped with F_4-TCNQ as the HIL, 1,1-bis-(di-4-tolylaminophenyl)cyclohexane (TAPS)[19] as the HTL, *N*,*N*′-dicarbazolyl-3,5-benzene (mCP)[19] doped with 10 wt. % *fac* tris(2-phenylpyridine) iridium ($Ir(ppy)_3$) green phosphorescent dopant as the EML,[20] 4,7-diphenyl-1,10-phenanthroline (BPhen) as ETL and BPhen doped with $CsCO_3$ electron injection layer.[18] The same anode and cathode structures as the fluorescent device were also employed.

The optical transmittance of the films were obtained by passing the white light from a Oriel Apex Monochromatic Illuminator through an Oriel Cornerstone 260 monochromator and using a Newport 818-UV photodetector to measure the monochromatic light intensity. The sheet resistance of the transparent electrodes was measured using the four-point probe technique. Luminance (*L*)–current density (*J*)–voltage (*V*) measurements were conducted in ambient conditions using an Agilent 4155C semiconductor parameter analyzer and the aforementioned Newport 818-UV photodetector. The luminance of the OLEDs was calibrated using a Konica Minolta LS-100 luminance meter assuming a Lambertian emission pattern. Electroluminescence (EL) spectra were taken using an Ocean Optics Jaz spectrometer. The power and external quantum efficiencies (η_P, and η_{EQE}, respectively) were derived based on published methods.[21]

3 Results and discusssion

3.1 Optical and Electrical Properties of the Multilayer Structures

Figure 2 shows the optical transmittance of the trilayer MoO_3/Au/MoO_3 structures with varying Au layer thicknesses as compared to that of the commercial ITO electrode. With a 5 or 10 nm thick Au layer, the trilayer structure can achieve a maximum transmittance of 85% to 90%, only slightly lower than that of the ITO. The transmittance of this trilayer structure does show stronger dependencies on the wavelength than the ITO, and the transmittance of trilayers with 5 to 10-nm thick Au intermediate layers is reduced to approximately 75% at 500 nm. The trilayer transmittance also shows a strong dependence on the Au layer thickness. While the structure with a 5-nm thick Au layer shows broad transmittance, as the Au layer thickness increases, a characteristic peak transmittance begins to form around 580 nm, and the overall transmittance of the structure steadily decreases, particularly for wavelength <500 nm.

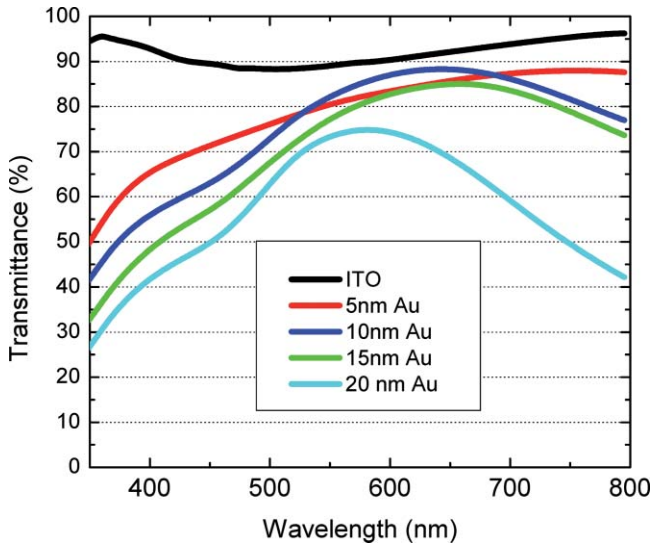

Fig. 2 Transmittance of the ITO and MoO_3/Au/MoO_3 electrode with various Au layer thickness.

Figure 3 shows the relationship between the transmittance (at 600 nm) and the sheet resistance for trilayers with varying Au layer thickness. While the 5-nm thick Au structure shows high transmittance, its sheet resistance (35 Ω/sq) was higher than that of ITO (~20 Ω/sq, approximately 120-nm thick). With a 10 nm or thicker Au intermediate layer, the sheet resistance of the trilayer is reduced to below 10 Ω/sq and decreases with the Au layer thickness, although this is accompanied by a simultaneous reduction in the optical transmittance. Therefore in order to apply this electrode to light-emitting devices, a balance between the transmittance and sheet resistance must be achieved. One important observation relates to the 10-nm sample, which possesses both sufficiently low sheet resistance (8.9 Ω/sq, much lower than that of the commercial ITO) and the highest transmittance at 600 nm. This phenomenon suggests a correlation between the more coherent Au layer and an optical enhancement perhaps related to surface plasmon resonance. This effect is further supported by the change in peak transmittance seen as the metal material is changed, suggesting a material dependent resonance. Figure 4 shows that by changing the metal intermediate layer used to Ag or using a sequentially deposited

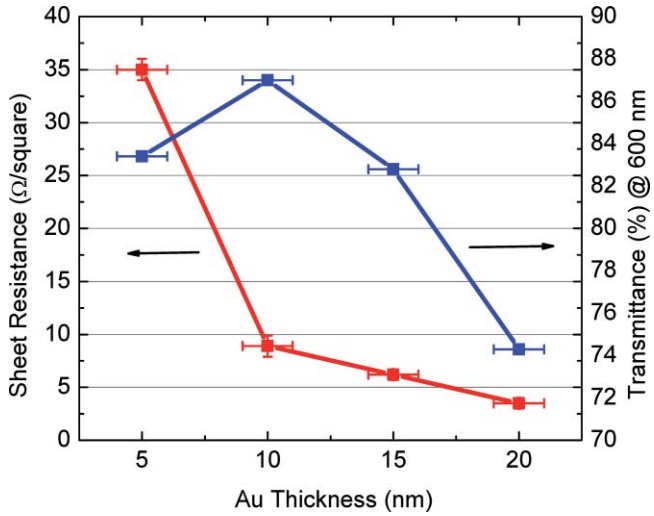

Fig. 3 Sheet resistance and transmittance at 600 nm as a function of Au layer thickness.

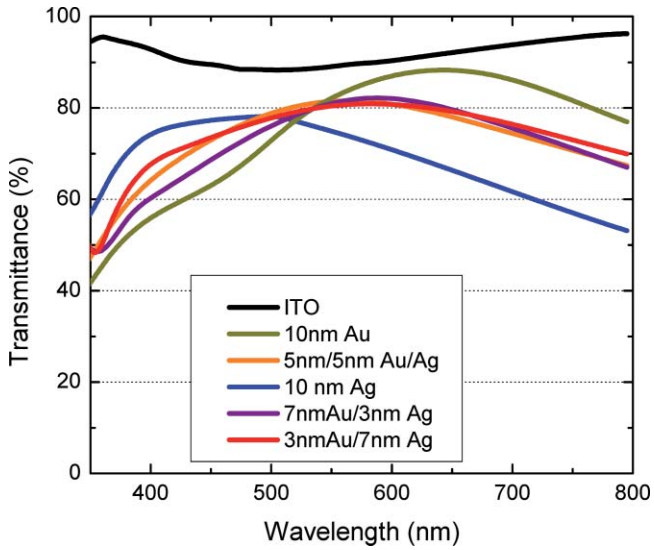

Fig. 4 Wavelength dependent transmittance of multilayer structures with Au, Au/Ag, and Ag intermediate layers.

Au/Ag bilayer structure, the maximum transmittance wavelength shifts from the red region of the electromagnetic spectrum to the blue (Ag) or green (Au/Ag) region. The 5nm/5nm or 3nm/7nm Au/Ag stacked interlayer structures appear to be more suited for white light-emitting devices as the corresponding transmittance is over 70% for the entire wavelength range of 450 to 650 nm, whereas either Ag or Au only results in a relatively poor transmittance at one end of the visible spectrum (long-wavelength end for Ag and short-wavelength end for Au). The transmittance of this stacked interlayer structure is close to the weighted average of the transmittances of the two components, although there are also variations due to uncertainties and reproducibility in the thicknesses of these ultrathin layers. Overall, this suggests that by adjusting the composition of the metal intermediate layer the transmittance of this transparent electrode structure can be tuned for a variety of niche applications and emissive molecules. It is also noted that the sheet resistance of the trilayer structures incorporating these Au/Ag composite intermediate layers is in the range of 12 to 16 Ω/sq, only slightly higher than that for the trilayer with a 10-nm thick Au intermediate layer (∼9 Ω/sq).

3.2 OLED Devices with Trilayer Transparent Electrodes

As this MoO_3/metal/MoO_3 trilayer structure shows promising electrical and optical properties, its application to OLED devices must also be examined. First, fluorescent devices were fabricated as previously described using the multilayer electrode with 10 nm Au as the intermediate layer. Figure 5(a) shows the *L-J-V* characteristics for the bottom-emitting Alq_3 device (with a commercial ITO anode) and its top-emitting counterpart with a MoO_3/Au/MoO_3 anode. The top-emitting device shows a somewhat lower current than the bottom-emitting device, especially at voltages just above the turn-on voltages of the devices (∼2.2 V). The inferior charge injection in the top-emitting device may not be entirely associated with the transparent trilayer electrode. More likely it could be due to the electron injection from the Al cathode. In a typical bottom-emitting structure, an interlayer of LiF or Cs_2CO_3 is first deposited onto the organic layer followed by an Al cathode, and reactions and diffusion may occur upon the deposition of hot Al atoms, which subsequently reduces the electron injection barrier.[22,23] When depositing a top-emitting structure with Al followed by an interlayer (such as Cs_2CO_3 used here), the same series of events may not occur. Nonetheless, the emission spectra of the bottom- and top-emitting

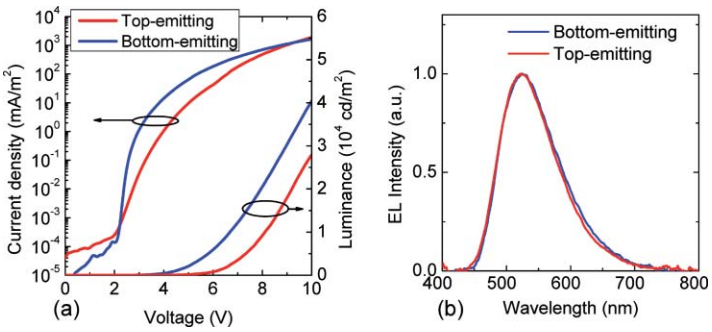

Fig. 5 (a) *L-J-V* characteristics of fluorescent bottom- and top-emitting devices. The commercial ITO anode was used in the bottom-emitting device whereas the MoO_3/Au/MoO_3 trilayer electrode was used as the anode in the top-emitting device. (b) EL spectra of the two devices.

devices as shown in Fig. 5(b) are nearly identical. This indicates that if the injection barrier can be overcome, the transmittance of this structure is unlikely to affect the emission of the device.

We also applied the trilayer transparent electrode to a *p-i-n* phosphorescent green-emitting device with both hole and electron injecting layers. The schematic energy level diagram of such devices is shown in Fig. 6(a). As shown in Fig. 6(b), the external quantum efficiency of the top-emitting device was mostly the same as that of the bottom-emitting device in the current density range of 0.1 to 100 mA/cm^2. The power efficiency of the top-emitting device however, shows a 20 to 30% reduction compared to the bottom-emitting device in this current density range, which is attributed to the somewhat higher drive voltage of the top-emitting device similar to the case of the fluorescent devices [Fig. 5(a)]. Based on this green *p-i-n* structure, the potential application of this electrode to high efficiency light emitting devices can be seen, so long as the high turn on voltage can be overcome.

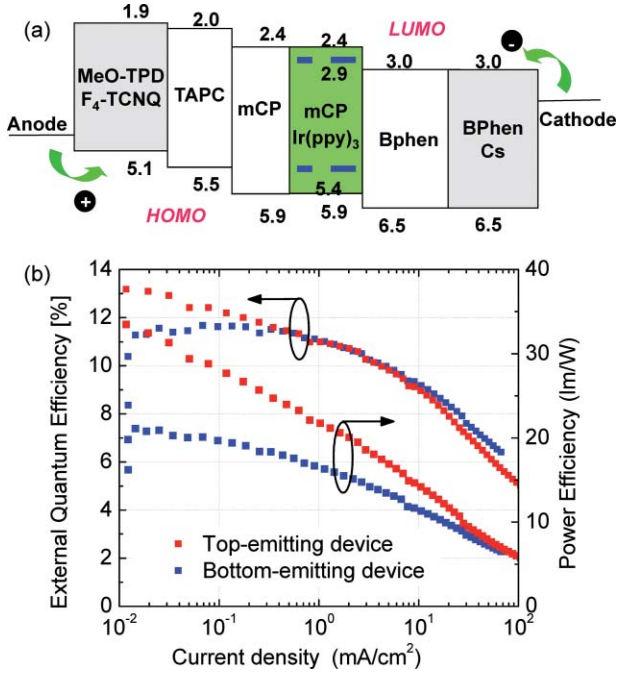

Fig. 6 (a) Energy level diagram of high efficiency *p-i-n* green phosphorescent devices; (b) external quantum and luminous power efficiencies of these two devices.

4 Conclusion

We have demonstrated a new architecture for a transparent multilayer electrode for use in thermally evaported top-emitting OLEDs. While its transparency is wavelength dependent, maximum transmittance up to 85% to 90% is achieved along with sheet resistances lower than typical commercial ITO electrodes. Furthermore, the wavelength dependence of the transmittance of such electrodes can be tuned based on the metal material used for the intermediate layer. When Au-containing multilayer structures were used as the anode in a top-emitting OLED, the emission spectra of the device matched that of the bottom-emitting devices with ITO anodes. These top-emitting devices also exhibit similar external quantum efficiencies as the bottom-emitting devices; however the somewhat inferior charge injection, likely caused at the Al cathode, leads to higher operating voltages and lower power efficiencies in the top-emitting devices. Further examination of these multilayer structures is clearly necessary as they present a promising avenue for the replacement of ITO in OLEDs.

Acknowledgments

The authors gratefully acknowledge financial support from the U.S. Department of Energy Solid State Lighting Program (Award No. 09EE0000990) and the Florida Energy Systems Consortium. S.H.E. also acknowledges a fellowship from Samsung SDI. Co., Ltd.

References

1. S. Reineke, F. Lindner, G. Schwartz, N. Seidler, K. Walzer, B. Lussem, and K. Leo, "White organic light-emitting diodes with fluorescent tube efficiency," *Nature (London)* **459**, 234–238 (2009).
2. E. F. Schubert and J. K. Kim, "Solid-state light sources getting smart," *Science* **308**, 1274–1278 (2005).
3. S. K. Park, J. I. Han, W. K. Kim, and M. G. Kwak, "Deposition of indium-tin-oxide films on polymer substrates for application in plastic-based flat panel displays," *Thin Solid Films* **397**, 49–55 (2001).
4. J. Xue, "Carrier transport in multilayer organic photodetectors: II. Effects of anode preparation," *J. Appl. Phys.* **95**, 1869–1877 (2004).
5. M.-H. Lu, M. S. Weaver, T. X. Zhou, M. Rothman, R. C. Kwong, M. Hack, and J. J. Brown, "High-efficiency top-emitting organic light-emitting devices," *Appl. Phys. Lett.* **81**, 3921–3923 (2002).
6. L. H. Smith, J. A. E. Wasey, and W. L. Barnes, "Light outcoupling efficiency of top-emitting organic light-emitting diodes," *Appl. Phys. Lett.* **84**, 2986–2988 (2004).
7. C.-C. Liu, S.-H. Liu, K.-C. Tien, M.-H. Hsu, H.-W. Chang, C.-K. Chang, C.-J. Yang, and C.-C. Wu, "Microcavity top-emitting organic light-emitting devices integrated with diffusers for simultaneous enhancement of efficiencies and viewing characteristics," *Appl. Phys. Lett.* **94**, 103302 (2009).
8. X.-W. Chen, W. C. H. Choy, S. He, and P. C. Chui, "Comprehensive analysis and optimal design of top-emitting organic light-emitting devices," *J. Appl. Phys.* **101**, 113107 (2007).
9. L. S. Hung, L. S. Liao, C. S. Lee, and S. T. Lee, "Sputter deposition of cathodes in organic light emitting diodes," *J. Appl. Phys.* **86**, 4607–4612 (1999).
10. Y. Abe and T. Nakayama, "Transparent conductive film having sandwich structure of gallium-indium-oxide/silver/gallium-indium-oxide," *Mater. Lett.* **61**, 3897–3900 (2007).
11. C. Guillén and J. Herrero, "Transparent conductive ITO/Ag/ITO multilayer electrodes deposited by sputtering at room temperature," *Opt. Commun.* **282**, 574–578 (2009).
12. K. S. Yook, S. O. Jeon, C. W. Joo, and J. Y. Lee, "Transparent organic light emitting diodes using a multilayer oxide as a low resistance transparent cathode," *Appl. Phys. Lett.* **93**, 013301 (2008).

13. S. Y. Ryu, J. H. Noh, B. H. Hwang, C. S. Kim, S. J. Jo, J. T. Kim, H. S. Hwang, H. K. Baik, H. S. Jeong, C. H. Lee, S. Y. Song, S. H. Choi, and S. Y. Park, "Transparent organic light-emitting diodes consisting of a metal oxide multilayer cathode," *Appl. Phys. Lett.* **92**, 023306 (2008).
14. S. Y. Ryu, S. J. Jo, C. S. Kim, S. H. Choi, J. H. Noh, H. K. Baik, H. S. Jeong, D. W. Han, S. Y. Song, and K. S. Lee, "Transparent organic light-emitting diodes using resonant tunneling double barrier structures," *Appl. Phys. Lett.* **91**, 093515 (2007).
15. S.-H. Eom, Y. Zheng, N. Chopra, J. Lee, F. So, and J. Xue, "Low voltage and very high efficiency deep-blue phosphorescent organic light-emitting devices," *Appl. Phys. Lett.* **93**, 133309 (2008).
16. J. Shi and C. W. Tang, "Doped organic electroluminescent devices with improved stability," *Appl. Phys. Lett.* **70**, 1665–1667 (1997).
17. C. W. Tang and S. A. VanSlyke, "Organic electroluminescent diodes," *Appl. Phys. Lett.* **51**, 913–915 (1987).
18. S.-H. Eom, Y. Zheng, E. Wrzesniewski, J. Lee, N. Chopra, F. So, and J. Xue, "Effect of electron injection and transport materials on efficiency of deep-blue phosphorescent organic light-emitting devices," *Org. Electron.* **10**, 686–691 (2009).
19. Y. Zheng, S.-H. Eom, N. Chopra, J. Lee, F. So, and J. Xue, "Efficient deep-blue phosphorescent organic light-emitting device with improved electron and exciton confinement," *Appl. Phys. Lett.* **92**, 223301 (2008).
20. M. A. Baldo, S. Lamansky, P. E. Burrows, M. E. Thompson, and S. R. Forrest, "Very high-efficiency green organic light-emitting devices based on electrophosphorescence," *Appl. Phys. Lett.* **75**, 4–6 (1999).
21. S. R. Forrest, D. D. C. Bradley, and M. E. Thompson, "Measuring the efficiency of organic light-emitting devices," *Adv. Mater.* **15**, 1043–1048 (2003).
22. H. Heil, J. Steiger, S. Karg, M. Gastel, H. Ortner, H. von Seggern, and M. Stoößel, "Mechanisms of injection enhancement in organic light-emitting diodes through an Al/LiF electrode," *J. Appl. Phys.* **89**, 420–424 (2001).
23. L. S. Hung, C. W. Tang, and M. G. Mason, "Enhanced electron injection in organic electroluminescence devices using an Al/LiF electrode," *Appl. Phys. Lett.* **70**, 152–154 (1997).

Edward Wrzesniewski is currently working toward his PhD in materials science and engineering at the University of Florida. He received his BS degree in materials science from Carnegie Mellon University in 2008. His current research work focuses on architecture modification and out coupling enhancements to organic light-emitting devices.

Sang-Hyun Eom received his BS (1999) from Hanyang University and his MS (2001) degrees from Pohang University of Science and Technology (POSTECH) majoring in mechanical engineering. He worked at Samsung SDI from 2001 to 2006 as a display device design engineer and joined the University of Florida in 2006 to pursue his PhD in materials science and engineering. His research at the University of Florida focuses on the development of high efficiency blue and white phosphorescent OLEDs and enhancing the light extraction efficiency in OLEDs. Upon completion of his PhD in December 2010, he returned to Samsung SDI, South Korea, where he is a senior research scientist in the Corporate R&D Center.

William T. Hammond received his MS (2007) and PhD (2011) degrees in materials science and engineering from the University of Florida. He also received a BS in physics from the College of William and Mary in 2005. His research work at the University of Florida focused on the design of new device structures and the development of new processing methods for both organic photodetectors and solar cells. Before coming to the University of Florida in 2006, he also worked in the Detector and Imaging Group at the Jefferson National Accelerator Facility in Newport News, Virginia to develop next-generation positron emission tomography (PET) imagers dedicated to the detection of breast cancer and heart disease.

Weiran Cao is a PhD candidate in materials science and engineering at the University of Florida. He received his BS degree in materials science from University of Science and Technology of China (USTC) in 2008. His current research work focuses on novel optical designs for organic light-emitting devices and photovoltaic cells.

Jiangeng Xue received his PhD in electrical engineering from Princeton University in 2005. He also received his BS (1995) and MS (1998) degrees in physics from University of Science and Technology of China (USTC). After working at Global Photonic Energy Corporation as a research scientist for nearly a year, he joined the University of Florida as an assistant professor in Materials Science and Engineering in 2005, and was promoted to associate professor in 2010. His research interests are broadly on the physics and processing of organic and hybrid organic–inorganic electronic materials and their applications in lighting, displays, photovoltaics, photodetection, and circuitry. He has about 50 journal publications and over 20 issued and pending patents.